Soil Dynamics and Earthquake Engineering 91 (2016) 160–174

Contents lists available at ScienceDirect

Soil Dynamics and Earthquake Engineering

journal homepage: www.elsevier.com/locate/soildyn

Experimental and conceptual evidence about the limitations of shear wave velocity to predict liquefaction

Ramón Verdugo

Principal of CMGI – Chile, Virginia Opazo 48, Santiago, Chile

ARTICLE INFO

Keywords:
Liquefaction
Shear wave velocity
Earthquake Geotechnical Engineering

ABSTRACT

Based on the liquefaction performance of sites with seismic activity, the normalized shear wave velocity, V_{s1}, has been proposed as a field parameter for liquefaction prediction. Because shear wave velocity, V_s, can be measured in the field with less effort and difficulty than other field tests, its use by practitioners is highly attractive. However, considering that its measurement is associated with small strain levels, of the order of 10^{-4}–10^{-3}%, V_s reflects the elastic stiffness of a granular material, hence, it is mainly affected by soil type, confining pressure and soil density, but it is insensitive to factors such as overconsolidation and pre-shaking, which have a strong influence on the liquefaction resistance. Therefore, without taking account of the important factors mentioned above, the correlation between shear wave velocity and liquefaction resistance is weak.

In this paper, laboratory test results are presented in order to demonstrate the significant way in which OCR (overconsolidation ratio) affects both shear wave velocity and liquefaction resistance. While V_s is insensitive to OCR, the liquefaction resistance increases significantly with OCR. In addition, the experimental results also confirm that V_s correlates linearly with void ratio, regardless of the maximum and minimum void ratios, which means that V_s is unable to give information about the relative density. Therefore, if shear wave velocity is used to predict liquefaction potential, it is recommended that the limitations presented in this paper be taken into account.

1. Introduction

Earthquakes of medium-to-large magnitude have systematically induced liquefaction in areas with sandy soil deposits. Recently, earthquakes in Chile 2010 (Mw=8.8), Japan 2011 (Mw=9.0) and New Zealand 2011 (Mw=6.3) have induced liquefaction of sands in many areas. As a consequence, these countries have had to manage the extensive damage of buildings, ports, dams, routes, lifelines, and bridges, along with the significant human and economic cost resulting from seismic events.

The state of the art and practice in geotechnical engineering provide analyses and methodologies to understand liquefaction phenomenon, as well as tools to predict the triggering of liquefaction. However, although the phenomenon is reasonably well understood, liquefaction is still one of the main sources of the large overall economic cost caused by earthquakes. Therefore, every effort should be made to develop new techniques and enhance existing methodologies for analyzing liquefaction, using theoretical and practical approaches. These efforts must account for the inherent difficulties faced on a daily basis by practitioners and researchers.

The assessment of liquefaction potential of loose saturated sandy soil deposits, soils with the highest liquefaction potential, can be done by retrieving "undisturbed" samples for laboratory tests; however, the successful completion of laboratory testing on this kind of soil is not always possible.

To overcome this situation there is a consensus in favor of field testing procedures that have the advantage of addressing the complexity of soils in their natural, undisturbed in-situ conditions.

In this context, the penetration resistances obtained by either Standard Penetration Tests (SPT) or Cone Penetration Tests (CPT), are well-accepted field parameters to characterize sandy soils and formulate significant correlations with the liquefaction resistance [1]. Figs. 1 and 2 present state-of-practice correlations between penetration resistances and cyclic resistances used in liquefaction analysis today.

Alternatively, the normalized shear wave velocity, V_{s1}, has been proposed as a field parameter for liquefaction prediction. The chart using V_{s1} is presented in Fig. 3. This chart uses the same framework of liquefaction charts developed based on the liquefaction performance of sites with seismic activities (Dobry et al. [2]; Robertson et al. [3]; Andrus et al. [4–6]; Dobry [7]).

Because the shear wave velocity correlates with the soil density, and because it can be measured in the field in a straightforward way, the V_s-

E-mail address: rverdugo@cmgi.cl.

http://dx.doi.org/10.1016/j.soildyn.2016.09.046
Received 12 February 2016; Received in revised form 25 September 2016; Accepted 27 September 2016
Available online 03 November 2016
0267-7261/

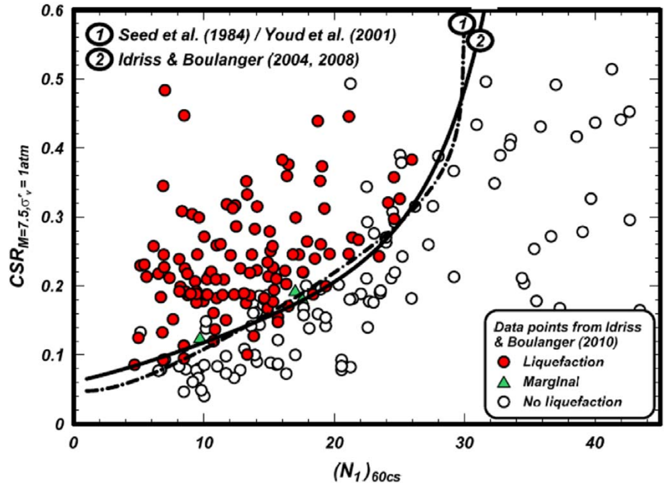

Fig. 1. Liquefaction chart based on SPT- $(N_1)_{60\ CS}$, M_w=7.5 [31].

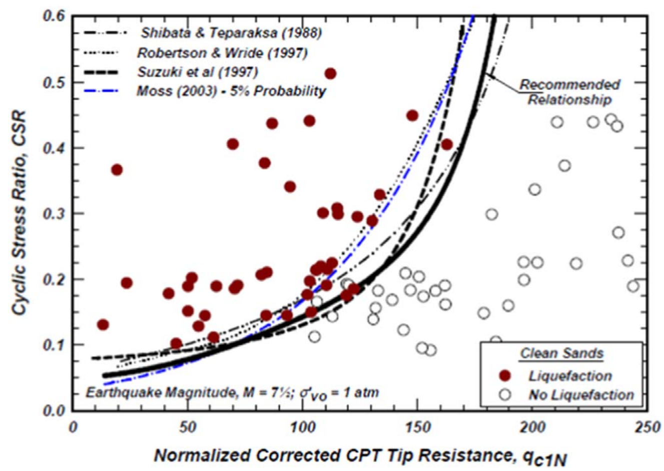

Fig. 2. Liquefaction chart based on tip resistance of CPT. M_w=7.5 ([41]).

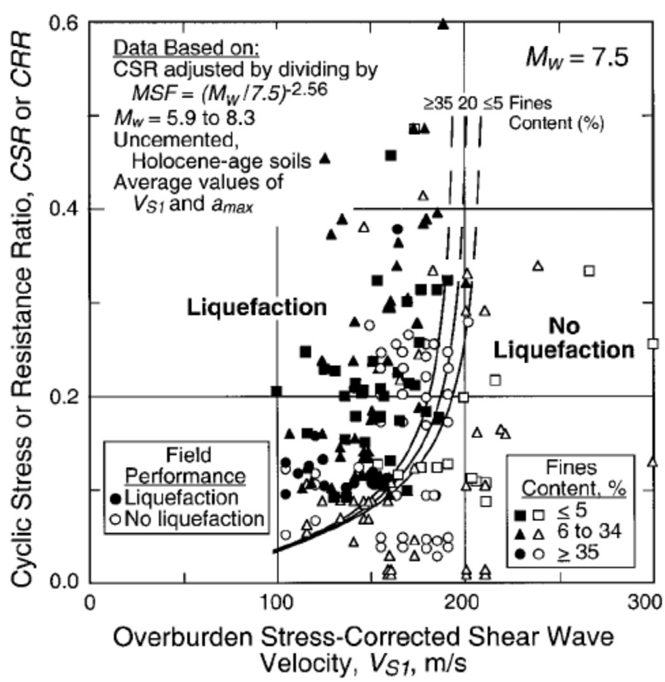

Fig. 3. Liquefaction chart based on shear wave velocity. M_w=7.5 [5].

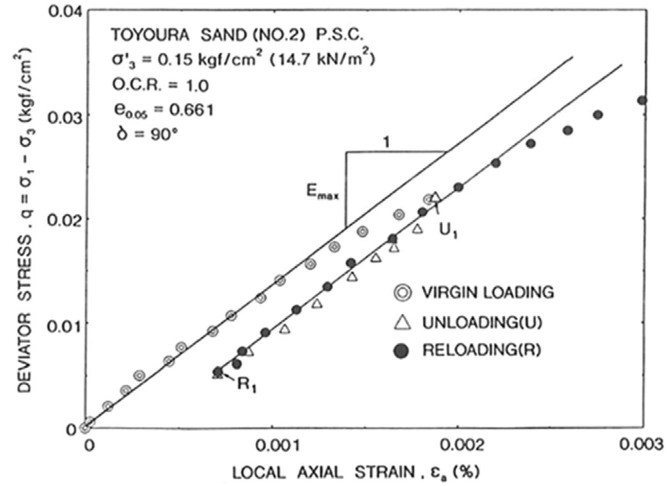

Fig. 4. Stress-strain curve showing elastic behavior for axial strain ≤10^{-3}% (shear strain ≤1.3×10^{-3}%) [10].

based procedures to evaluate liquefaction resistance are of great interest and naturally attractive to geotechnical engineers. Despite its appealing features for engineering practice, there is an important concern that arises in the use of V_s as a liquefaction predictor. The shear wave velocity measurements are associated with small strain levels, of the order of 10^{-4}–10^{-3}%. Therefore, this parameter can only capture elastic soil properties and is unlikely to be sensitive to factors that affect liquefaction, which is a large strain phenomenon (Jamiolkowski et al. [8]; Verdugo, [9]).

Based on this concern, the present paper discusses the intrinsic limitations of the use of the shear wave velocity as a liquefaction predictor.

2. Shear strain levels and behavior of sandy soils

Depending on the shear strain level that an element of sandy soil experiences, the mechanical behavior could be significantly different. For shear strains below 10^{-5} (10^{-3}%), the stress-strain response is fairly linear, as shown by the experimental results obtained by Tatsuoka et al. [10], and presented in Fig. 4. This observation is also supported by the rather limited degradation experienced by the shear modulus of sands in this range of shear strains, as depicted in Fig. 5 (Kokusho [11]).

For shear strains greater than 10^{-5} (10^{-3}%), sandy soils show an elasto-plastic behavior, where both permanent and recoverable mechanical strains are observed after unloading. In this scenario, plastic deformations take place, even though no volumetric strain accumulations are observed up to a strain level of the order of 10^{-4} (10^{-2}%).

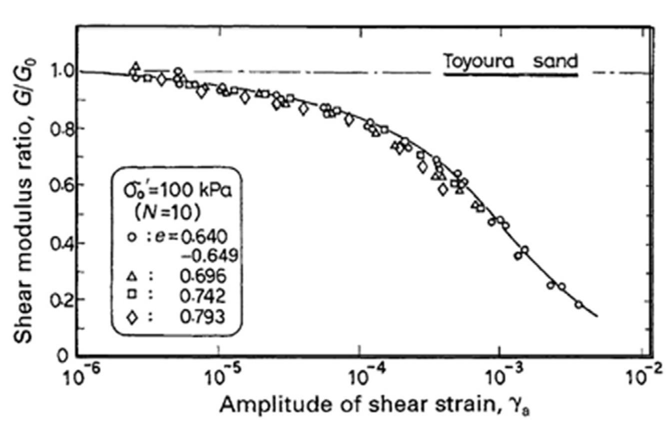

Fig. 5. Typical degradation curves of shear modulus for Toyoura sand [11].

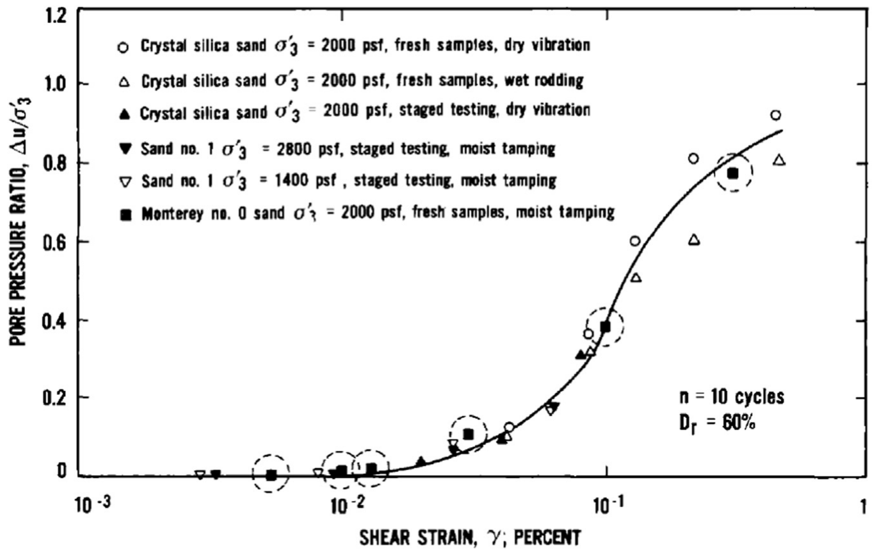

Fig. 6. Experimental evidence about the threshold strain [12].

Based on experimental evidence and theoretical considerations, Dobry et al. [12] introduced the concept of "threshold strain". This parameter separates the cyclic response of the soil with and without volumetric strain accumulations. This concept has been supported by several studies that have provided clear experimental evidence on the existence of this limit strain, below which soils do not present volumetric strain accumulations (Dyvik et al. [13]; Vucetic [14]; Dobry et al. [15]). This singular strain level has been renamed as "volumetric threshold shear strain" to emphasize that this threshold relates to the volumetric strains. Fig. 6 shows experimental results supporting the existence of this threshold strain. From these experimental data, shear strains of the order of 10^{-2}% can be identified as a limit shear strain value.

For shear strain levels higher than of the order of 10^{-3} (10^{-1}%), the strain rate effect appears. In this case, the loading speed alters the stiffness as well as the strength of the soil (Ishihara, [16,17]). The experimental evidence shows that the strain rate effect is significant in clayey materials but not significant in sandy soils.

Under cyclic loadings that induce shear strain levels larger than 10^{-2} (1%), the mechanical properties of the soil are significantly affected, and the soil experiences noticeable changes in response to the progression of the cycles. Fig. 7 shows an example of this behavior (Towhata, [18]); after each cycle of loading, a clear modification of the stress-strain loop is observed. The magnitude of the changes associated with the progress of cycles is most relevant in loose sandy soils, in which important rearrangement of particles takes place.

The thresholds described above have to be understood as the transition points around which the mechanical behavior of the soil is gradually modified. Fig. 8 shows a summary of the main characteristics of the mechanical behavior of sandy soils, which can be associated with the shear strain level.

On the other hand, measurements of the shear wave velocity are associated with shear strain levels in the range of 10^{-6} to 5×10^{-5}, where sandy soils do not present volumetric strain accumulation, nor significant plastic deformations. The shear wave velocity is a linear-elastic soil parameter, related to the maximum soil stiffness at a particular state of stress. In this regard, V_s should not be capable of capturing the potential of volumetric strains of sands, which manifest themselves at large strains after significant change in the state of stress.

3. Liquefaction phenomenon

The liquefaction phenomenon is intrinsically related to the natural tendency of loose sands, and low plasticity silty-sands, to experience positive volumetric strains (contraction) when subjected to either monotonic or cyclic loading. When the applied loads are fast enough, as compared to the drainage capacity of the soil, the potential volumetric strains are impeded in their development, and this does develop pore water pressures.

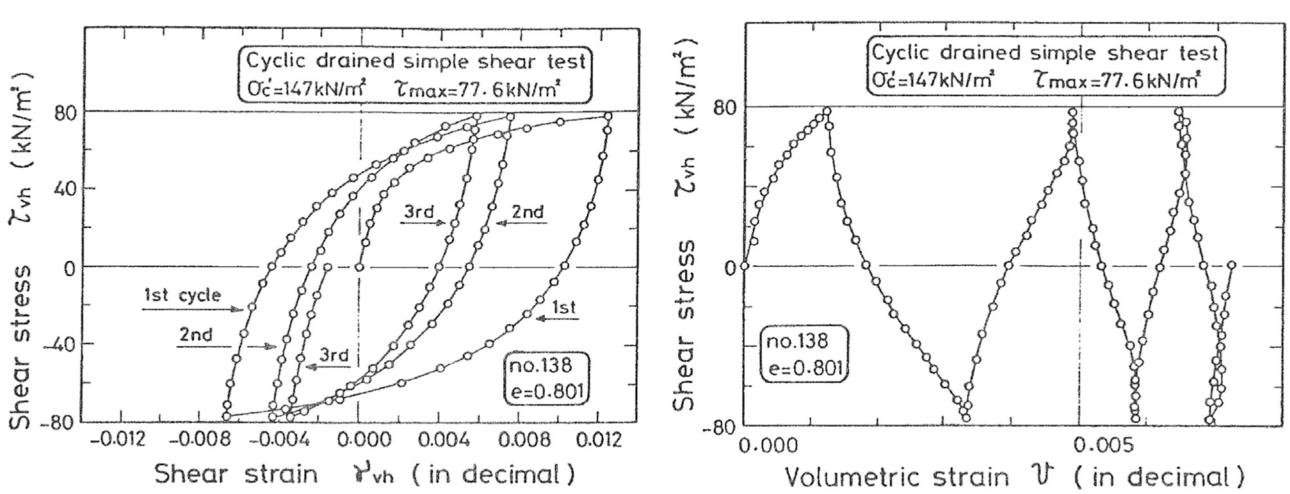

Fig. 7. Cyclic soil response for maximum shear strain level larger than 1% [18].

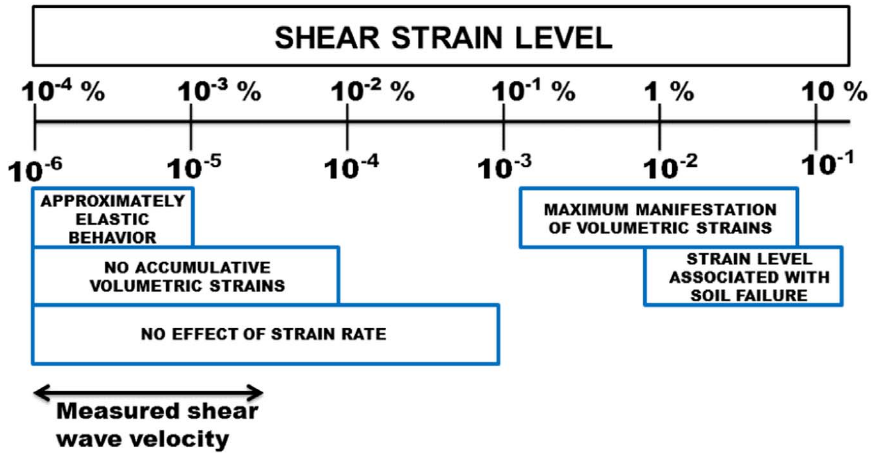

Fig. 8. Shear strain level and characteristic behavior of cohesionless soils.

Depending on the field conditions, two scenarios for the occurrence of liquefaction are possible: (1) a flow failure type, in which driving shear forces are larger than the post-liquefaction strength (residual undrained strength), and (2) cyclic softening of level ground.

Loose saturated cohesionless soils may undergo a liquefaction-induced flow failure type, characterized by a sudden loss of strength and the subsequent flow of the soil mass in a short period of time. This kind of failure can be triggered not only by earthquakes but also by disturbances that are quick enough to induce an undrained response (Casagrande [19]; Ishihara [20]; Verdugo [21], Verdugo and Ishihara [22], among others). Fig. 9 shows the contractive response of a sand tested in undrained conditions. In this test, the initial static deviator stress is greater than the ultimate undrained shear strength. As a consequence, a flow failure is developed. In this test, the observed drop in shear strength starts at an axial strain level which is greater than 0.5%.

In the case of the level ground type of failure, loose saturated cohesionless soils subjected to cyclic seismic loadings may experience important pore pressure buildup, causing a systematic reduction of the soil stiffness, or cyclic softening. Additionally, the most common outcome of the large buildup of excess pore pressure is the action of seepage forces that induce upward flow. This flow can transport soil particles to the ground surface, generating sand boils, typically in a volcano shape.

The available experimental information indicates that liquefaction resistance is controlled by factors that also influence the penetration resistance, which may explain the success of the penetration-based charts for predicting liquefaction resistance [15].

4. Main features of the standard penetration test

The SPT blow count provides the penetration resistance of the soil, associated with its failure. Therefore, in this field test, the granular material is forced to mobilize all its available shear strength. The SPT is considered a partially drained test; experimental results obtained using a small tank suggest that the excess pore pressure generated during the SPT depends on the velocity of blow application, as illustrated in Fig. 10 (Verdugo et al. [23]). According to these experimental data the SPT N-value tends to reflect the undrained soil response.

Despite the non-negligible deficiencies of the SPT, this field test continues to be significantly used by the geotechnical community around the world. Additionally, due to its application as an index for liquefaction resistance, efforts to improve its standardization have been made. Accordingly, the SPT blow count normalized to an overburden pressure of 1 ton/ft^2 (1.08 kg/cm^2≈100 kPa) and a hammer energy ratio of 60%, $(N_1)_{60}$, has been introduced (Seed et al. [24]). Additional corrections include factors for borehole diameter, rod length and sampler with or without a liner (Youd et al. [1]). The SPT-based procedure was the first method empirically developed for predicting the initiation of earthquake-induced liquefaction of sands. It was started by Kishida [25] and Ohsaki [26] who observed the liquefaction-induced failures during the 1964 Niigata Earthquake. The procedure was consolidated by Seed and co-investigators (Seed et al. [27,28,24]) by analyzing actual case histories with and without liquefaction. The SPT-based procedure has been confirmed and improved by several studies, adding case histories provided by recent large earthquakes ([1,29,15,30,31], among others).

Since the experimental work carried out by Gibbs and Holtz [32],

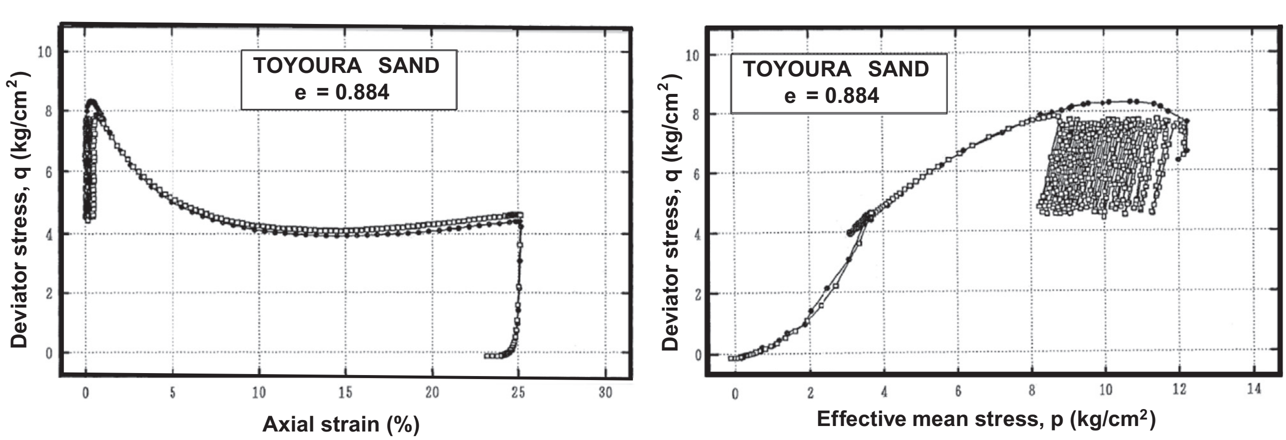

Fig. 9. Undrained soil response with strength drop [9].

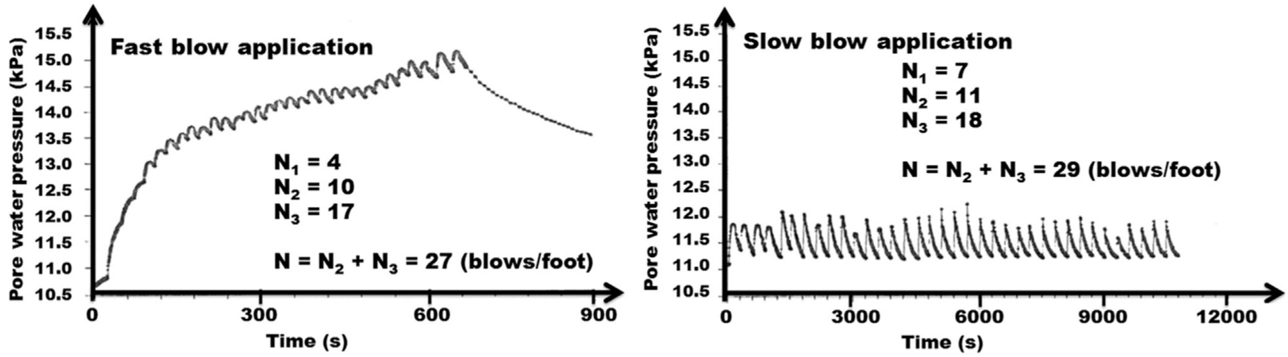

Fig. 10. Effect of blow velocity on the excess pore water pressure during SPT.

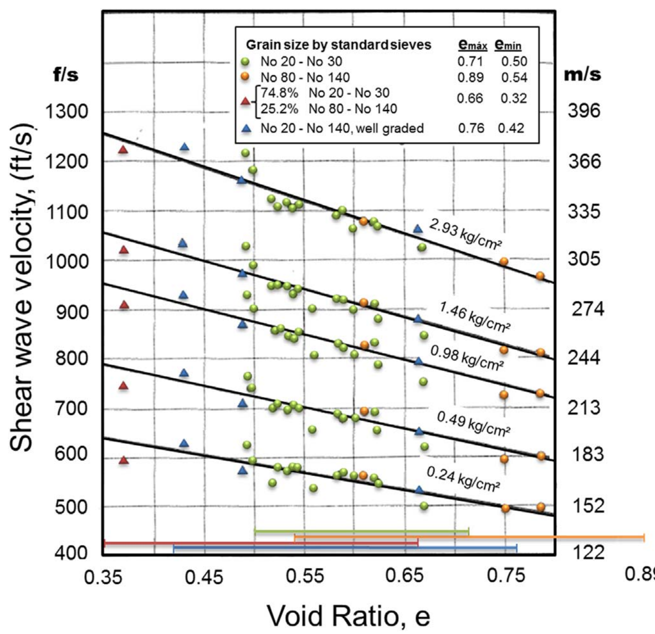

Fig. 11. Shear wave velocity vs void ratio (modified from [51]) 1 kg/cm^2 to 100 kPa.

empirical correlations between the SPT N-value, the vertical effective stress, and the relative density have been proposed (Cubrinovski et al. [33]). A comprehensive study by Skempton [34] observed that the SPT N-value varies with the relative density, D_r, and the vertical effective stress, σ'_v, according to the expression:

$$N = (a + b \cdot \sigma'_V) \cdot D_r^2 \tag{1}$$

where a and b are constants for a given kind of sand. These values tend to increase with the grain size, aging, and over-consolidation ratio. It is important to mention that the value of constant "b" depends on the adopted units of σ'_v. Following the original work of Skempton [34], these units are (kg/cm^2) for the vertical effective stress, σ'_v, and therefore, 1/(kg/cm^2) for b. The relative density, D_r, is expressed as a ratio (not as a percentage). Considering the energy correction (60%) and the normalization at σ'_v=1 kg/cm^2 (≈1 ton/sq ft ≈1 atm≈1 bar≈100 kPa), the previous relationship becomes:

$$(N_1)_{60} = (a + b) \cdot D_r^2 \tag{2}$$

Therefore:

$$(N_1)_{60} = \frac{a/b + 1}{a/b + \sigma'_V} N_{60} \tag{3}$$

According to the experimental data from Skempton [34], for normally consolidated sands, the ratio a/b varies roughly between 1 and 2. However, for overconsolidated fine sands, this ratio varies between 0.6 and 0.8. Youd and co-workers recommend to adopt a/b=1.2, considering the good fit with the original curve proposed by Seed and Idriss [35] for normalizing the SPT N-value to σ'_v=1 bar (Kayen et al. [36]; Youd et al. [1]). Therefore, for normally consolidated and overconsolidated sands, the following expressions can be consid-

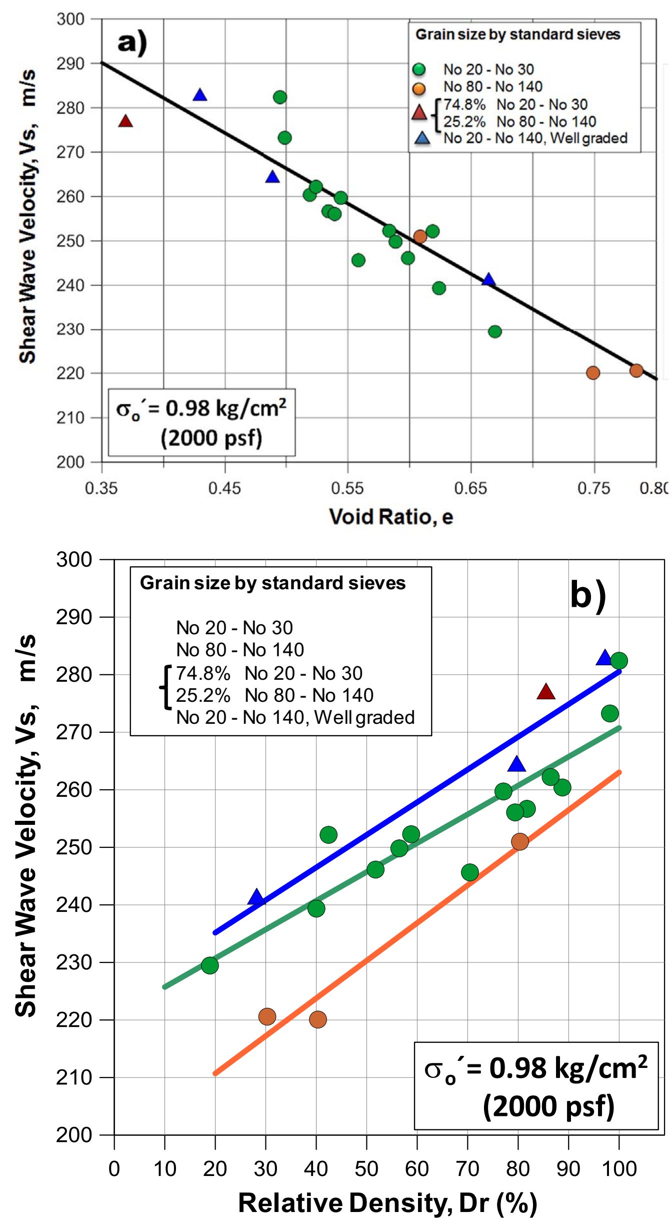

Fig. 12. Shear wave velocity as function of (a) void ratio and (b) relative density (data from [51]) 1 kg/cm^2 to 100 kPa.

Table 1
Physical properties of tested sands.

Sand	Grain shape	D_{50} (mm)	FC (%)	G_s	e_{max}	e_{min}
Sand S	Subangular to angular	0.15	7	2.60	0.862	0.505
Sand C	Angular	0.15	0	2.72	1.147	0.664

FC: Fines content; Gs: Specific gravity; D_{50}: medium grain size.

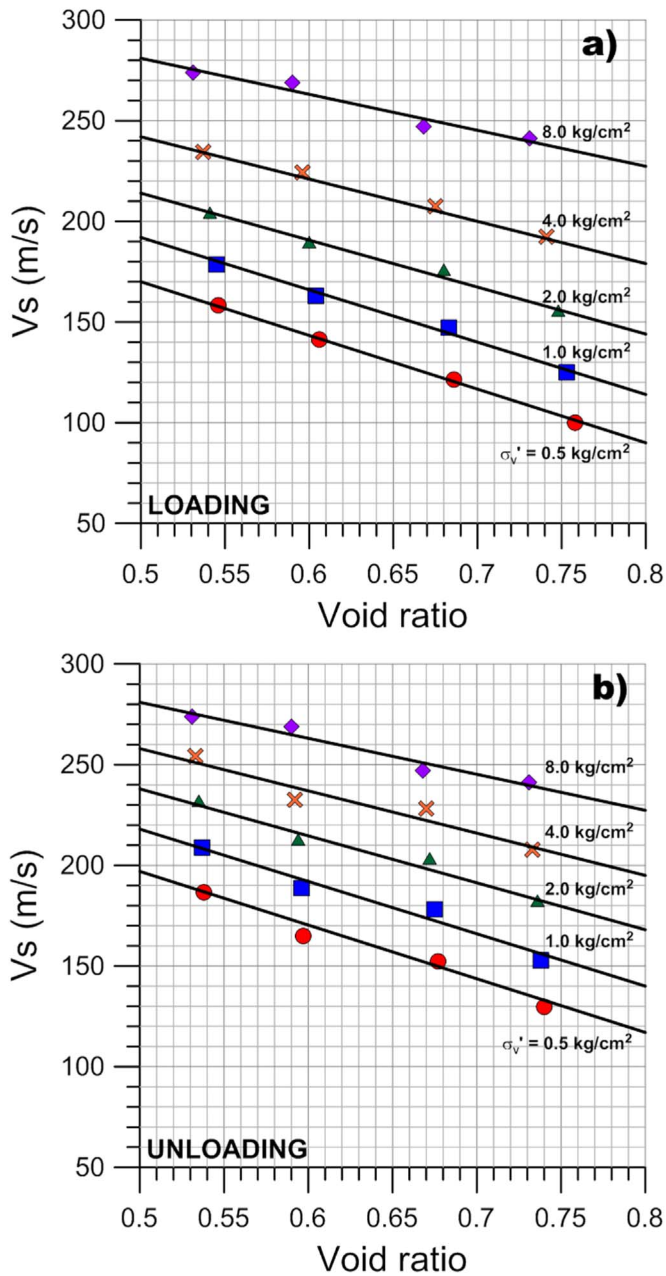

Fig. 13. Shear wave velocities of Sand S measured during (a) loading and (b) unloading (1 kg/cm^2 to 100 kPa).

ered:

$$(N_1)_{60} = \frac{2.2}{1.2 + \sigma_V'} N_{60} \quad \text{(Normally Consolidated Sands)} \tag{4}$$

$$(N_1)_{60} = \frac{1.7}{0.7 + \sigma_V'} N_{60} \quad \text{(Overconsolidated Sands)} \tag{5}$$

For normally consolidated natural sandy soil deposits, Skempton [34] found that the sum (a+b), or the quotient $(N_1)_{60}/D_r^2$, has an average value of around 60, so that:

$$(N_1)_{60} \approx 60 \cdot D_r^2 \tag{6}$$

In the case of overconsolidated sandy soil deposits, the SPT N-value is significantly influenced by the horizontal effective stress, which is a function of the OCR. In any case, for heavily overconsolidated sands, K_0 is not greater than one (Jamiolkowski et al. [37]), which results in the following approximation, for overconsolidated sands:

$$(N_1)_{60} \approx 73 \cdot D_r^2 \tag{7}$$

These empirical expressions are the outcome of the following facts: $(N_1)_{60}$ is strongly influenced by the relative density and the ground stress history, and $(N_1)_{60}$ correlates with the soil shear strength. Consequently, the use of $(N_1)_{60}$ as a liquefaction predictor makes sense. Nevertheless, it is important to point out that there are a significant number of experimental results and in-situ measurements suggesting that the aforementioned relationships may vary according to the sand types, which can be seen as a weakness of the SPT to be used without limitations. Furthermore, SPT can be substantially affected by an inappropriate execution of the borehole, where the tested soil may already be disturbed by the borehole operation.

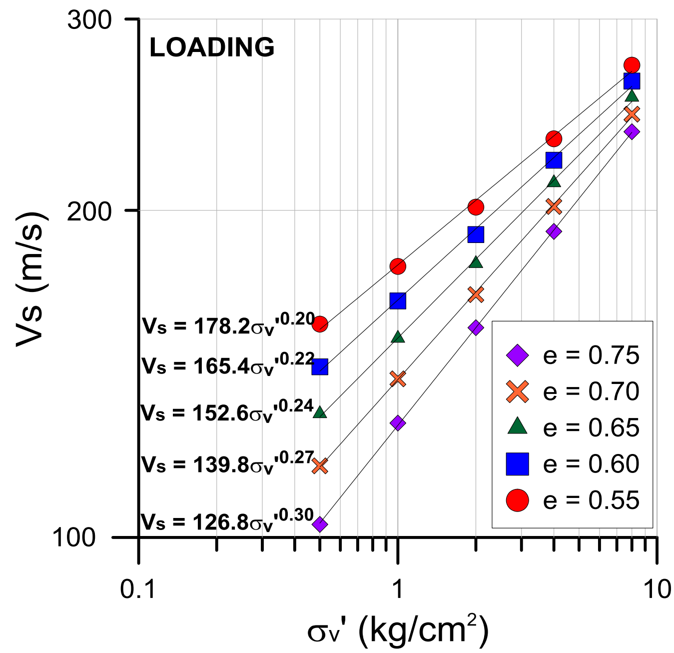

Fig. 14. Vs of Sand S as function of the vertical pressure for given void ratios (1 kg/cm^2 to 100 kPa).

5. Main features of the cone penetration test

The use of CPT and its popularity in geotechnical engineering practice have grown all around the world due to the significant amount of research that has become available. This work has encouraged significant progress in electronic tools as well as in the development of semi-empirical methodologies to estimate different soil parameters. The CPT has several advantages over the SPT. For example, the CPT provides nearly continuous data, it has a well-defined standardized procedure for its implementation, measurements and test result analysis, and it produces repeatable test results. It is widely recognized that in sandy soils with low fines contents, the cone penetration obtained at the standard rate of 2 cm/s generates a drained soil response. Therefore, at the standard velocity of penetration, CPT reflects the mobilized drained strength of sandy soils, according to their in-situ state of stresses and packing.

The CPT-based procedure to evaluate the liquefaction resistance of

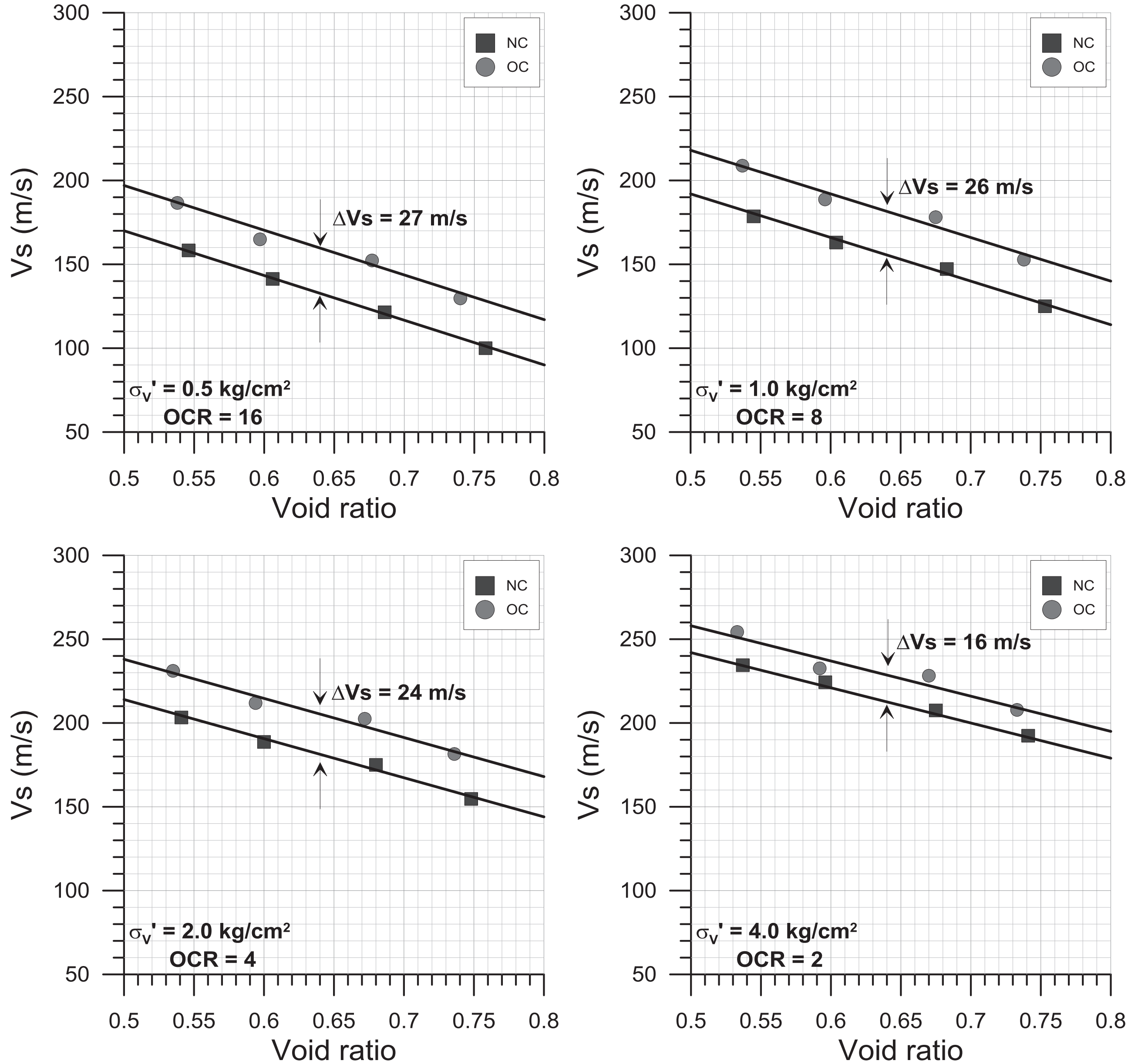

Fig. 15. Vs of Sand S measured at different vertical stresses and overconsolidation ratios (1 kg/cm^2 to 100 kPa).

sands was developed by replacing the corrected standard penetration resistance $(N_1)_{60}$ by the corrected tip resistance q_{1c} (Stark et al. [38]; Robertson et al. [39]; Youd et al. [1]; Suzuki et al. [40]; Idriss et al. [41]). Basically using calibration chamber tests, a relationship between CPT tip resistance, q_c, vertical effective stress and relative density has been developed (Schmertmann. [42]; Lunne et al. [43]; Baldi et al. [44]; Jamiolkowski et al. [37], among others). However, it has been pointed out that factors such as sand compressibility, age, and stress history may affect this type of correlations, making them not unique (Robertson et al. [45]; Bellotti et al. [46]). For normally consolidated, unaged and uncemented sandy soil deposits, the following expression has been proposed:

$$q_c = c_O \cdot P_a \cdot \left(\frac{\sigma'_V}{P_a}\right)^{C_1} \exp^{(C_2 \cdot Dr)} \tag{8}$$

where c_o, c_1 and c_2, are empirical non-dimensional coefficients. P_a is the atmospheric pressure expressed in the same unit of the vertical stress and tip penetration resistance. Relative density is expressed as a fraction of the unity.

Analogously, a normalized tip resistance, q_{c1}, at σ'_v=100 kPa (1 atm) is defined:

$$q_{c1} = c_O \cdot P_a \cdot \exp^{(C_2 \cdot Dr)} \tag{9}$$

Therefore:

$$q_{c1} = \frac{q_C}{\left(\frac{\sigma'_V}{P_a}\right)^{C_1}} \tag{10}$$

A comprehensive investigation performed by Jamiolkowski and co-workers (Jamiolkowski et al. [47]) using silica sands (Ticino, Toyoura and Hokksund sands), permitted the establishment of the following relationship between CPT tip resistance, q_c, vertical effective stress and relative density, for normally consolidated, unaged sands:

$$q_c = 17.68 \cdot P_a \cdot \left(\frac{\sigma'_V}{P_a}\right)^{0.5} \exp^{(3.1 \cdot Dr)} \tag{11}$$

Then, for σ'_v=1 atm (100 kPa):

$$q_{c1} = 17.68 \cdot P_a \cdot \exp^{(3.1 \cdot Dr)} \tag{12}$$

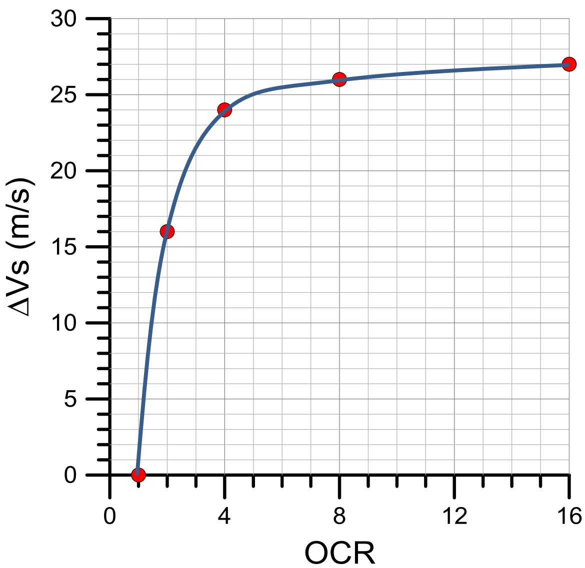

Fig. 16. Increment of shear wave velocity of Sand S due to overconsolidation.

In the case of overconsolidated sands, Jamiolkowski and co-workers proposed to replace the vertical stress by the mean stress, σ'_m, and assume K_0=1. For overconsolidated silica sands, the previous relationship becomes [47]:

$$q_c = 24.94 \cdot P_a \cdot \left(\frac{\sigma'_V}{P_a}\right)^{0.46} \exp^{(2.96 \cdot Dr)} \tag{13}$$

These empirical expressions show that the CPT tip resistance is strongly influenced by the relative density, and also by the stress history of the soil. Also, the CPT tip resistance correlates with the drained shear strength. These facts give the conceptual support for using the CPT tip resistance as a liquefaction predictor. Again it is important to point out that there are experimental results indicating that the above relationships may vary according to the sand types and permeability, which is also a warning to use the CPT with a full understanding of its limitations.

6. Normalized shear wave velocity

The shear wave velocity, V_s, measured either in the field or the laboratory, is an important material property that is directly related to the soil stiffness at a small strain level. In the field, V_s can be measured by different methods such as down-hole, cross-hole, suspension logging and surface wave methods. In the laboratory, it can be measured using resonant column tests, bender elements, and compression tests implemented with local strain transducers. Due to these existing methods for measuring V_s, this property is especially attractive for characterizing soils that are difficult to sample, like saturated loose sandy materials. This real advantage is probably the most important attribute promoting the use of V_s to predict liquefaction potential.

Experimental results have shown that V_s is a function of the principal stresses acting in the directions of wave propagation and particle motion, and is insensitive to the out-of-plane principal stress (Roesler [48]; Stokoe et al. [49]; Belloti et al. [50]; among others). Based on empirical evidence, V_s is given by:

$$V_S = A \cdot F(e) \cdot \left(\frac{\sigma'_a}{P_a}\right)^m \cdot \left(\frac{\sigma'_b}{P_a}\right)^n \tag{14}$$

where A is a soil property parameter, in units of velocity. F(e) is the void ratio function, while σ'_a and σ'_b represent the principal effective stresses in the direction of the wave propagation and particle motion, respectively. P_a is the atmospheric pressure expressed in the same units as σ'_a and σ'_b. The parameters n and m are dimensionless exponents.

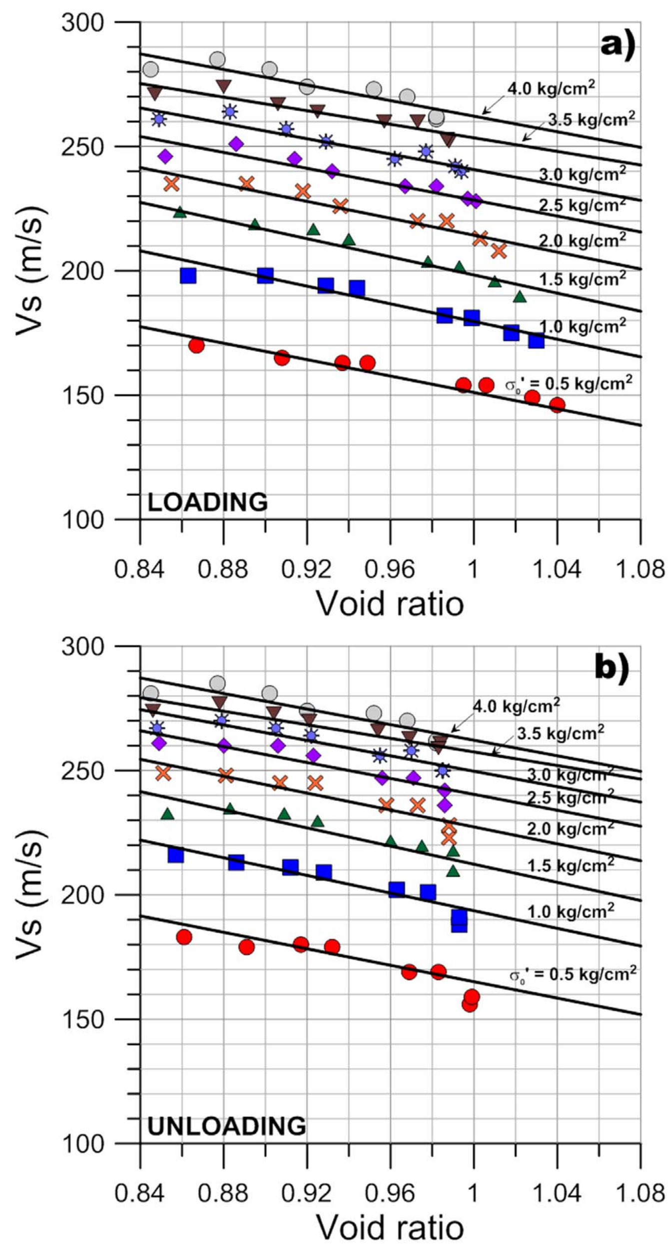

Fig. 17. Shear wave velocities of Sand C measured during (a) loading and (b) unloading (1 kg/cm² to 100 kPa).

When V_s is measured for a condition of either vertical wave propagation or vertical particle motion, the vertical and horizontal effective stresses can be associated with σ_a and σ_b, respectively. Additionally, the horizontal and vertical effective stresses are related through the coefficient of earth pressure at rest, K_o. Without loss of generality in the analysis, according to reported data, the values of m and n can be fixed equal to 0.125. Thus, the expression for V_s becomes:

$$V_S = A \cdot F(e) \cdot K_O^{0.125} \cdot \left(\frac{\sigma'_V}{P_a}\right)^{0.25} \tag{15}$$

Introducing the normalized shear wave velocity, V_{s1}, which is associated with a vertical effective stress σ'_v=1 kg/cm^2 (100 kPa) the following expression is obtained:

$$V_{S1} = A \cdot F(e) \cdot K_O^{0.125} \tag{16}$$

Therefore,

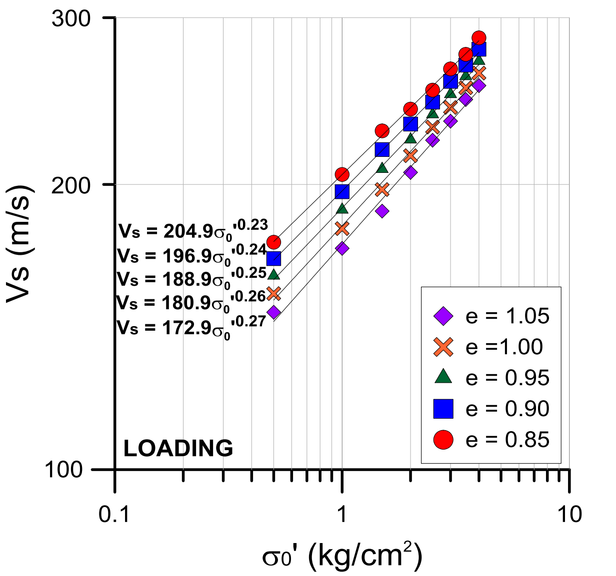

Fig. 18. Vs of Sand-C as function of the confining pressure for given void ratios (1 kg/cm^2 to 100 kPa).

$$V_{S1} = V_S\left(\frac{P_a}{\sigma'_V}\right)^{0.25} \tag{17}$$

The chart used for liquefaction evaluation, based on the shear wave velocity, uses the normalized shear wave velocity, V_{s1}. Its philosophy follows the empirical approach of both the SPT and the CPT-based procedures used to evaluate the earthquake-induced liquefaction of sands.

From a general point of view, the V_{s1}-based chart (Fig. 3) has at least two serious weaknesses. First, it presents an important number of data points that can be identified as false positives, in the sense that they plot significantly above the curve established as a frontier separating liquefaction from no-liquefaction, which generates a reasonable doubt about the actual existence of this frontier. Second, for values of V_{s1} greater than, say 180 m/s, the proposed frontiers for the three levels of fines become extraordinarily steep, which is unrealistic. For instance, for sands with fines content in the range of 5–35%, a change of V_{s1}, from 190 to 200 m/s, the Cyclic Resistance Ratio (CRR) would increase from 0.21 to about 0.45 or more. This means that for values of V_{s1} larger than 180 m/s, the evaluation of CRR is unrealistically sensitive to small variation of V_{s1}. Furthermore, shear wave velocities of thin layers of loose sands may not be obtained appropriately because they may be hidden by denser layers. This represents a serious weakness considering the high sensitivity of CRR with respect to V_{s1}.

7. Shear wave velocity and void ratio

The pioneering experimental work carried out by Hardin and Richart [51], using different gradations of Ottawa sand, concluded that V_s decreases linearly with increasing void ratio. Fig. 11 shows the experimental data from Hardin and Richart [51]. At the bottom of the plot, the intervals between e_{max} and e_{min} of each grading have been added as shown in this figure. The V_s was found to be independent of the grain size, grading, and relative density of the sand. This feature is critical, and needs analyzing in greater depth due to the impact it may have on the real capability of V_s as a predictor of liquefaction.

From Figs. 11 and 12a, it seems that V_s is closely related to void ratio, but V_s is not uniquely correlated to relative density. This observation is confirmed in Fig. 12b, where the same original data of V_s, for a confining pressure of 0.98 kg/cm^2 (2000 psf ≈100 kPa), have been re-plotted in terms of relative density. It is observed that the single relationship governed by the void ratio is divided into new relationships for each sample of Ottawa sand.

It is important to note the enormous range of relative densities that result in the same V_s (Fig. 12b). For example, Ottawa sand No. 20 to No. 140, at a relative density of 30%, has a V_s of around 240 m/s, and Ottawa sand No. 80 to No. 140, at a relative density of 64%, has similar V_s of around 240 m/s.

All the experimental evidence reported consistently indicates that V_s is a function of the void ratio, being expressed through the void ratio function, $F(e)$, previously introduced. The experimental data show that V_s is not especially affected when close to the maximum and minimum void ratios (see Fig. 11). This implies that V_s is unable to discriminate whether the soil packing is dense or loose. This inherent feature of V_s is a clear limitation on the use of this parameter in analyses where the soil response is strongly dependent on the relative density, as in the case of liquefaction phenomenon.

8. Effect of overconsolidation on the shear wave velocity

Bender element tests were carried out on two types of sand to evaluate the impact of the mechanical overconsolidation on the shear wave velocity of sands. The first sand was from Sweden, denoted as Sand-S, while the other was from Chile, denoted as Sand-C. While Sand-S is a natural sand, Sand-C is a copper tailings material retrieved from a tailings dam and washed through sieve #200 (ASTM) to eliminate any fines. Table 1 presents the main physical properties of the sands investigated.

The shear wave velocity measurements of sand-S were carried out by the author in the geotechnical laboratory of the Norwegian Geotechnical Institute, in 1996. The tests were performed on sands deposited in a consolidation cell equipped with bender elements [52].

The specimens were vertically loaded at a stress of 0.5 kg/cm^2 (50 kPa) and then saturated. Afterwards, vertical pressures of 1, 2, 4, and 8 kg/cm^2 were applied on the sand specimens. A subsequent unloading process was performed, decreasing the load from 8 kg/cm^2, in steps of 0.5 kg/cm^2, to generate over-consolidation ratios varying from 1 to 16. The shear wave velocity was measured at each state of stress induced by the loads.

The shear wave velocities of sand-C were measured in the geotechnical laboratory of University of Chile [53]. The sandy soil specimens were prepared in triaxial cells equipped with bender elements. The samples, 10 cm high and 5 cm in diameter, were saturated (B-value greater than 0.95) and isotropically consolidated at effective confining pressures of 0.5, 1.0, 1.5, 2.0, 2.5, 3.0, 3.5 and 4.0 kg/cm^2. Afterwards, the specimens were unloaded, following the same steps. At each effective confinement, for both loading and unloading, the shear wave velocities of the specimens were measured.

Fig. 13 shows the linear plot of the shear wave velocities as a function of the void ratio, for various vertical stress levels (0.5, 1, 2, 4, and 8 kg/cm^2), measured on Sand-S specimens during the loading and unloading stages.

For both stages of loading and unloading of the specimens, the plots in Fig. 13a and b show that (1) V_s increases with the confinement and that (2) V_s decreases as the void ratio increases, regardless of the confinement. These observations are in agreement with previous studies that highlighted the effect of both the confinement and void ratio on the shear modulus.

From Fig. 13a, the values of V_s were obtained at various effective confining pressures and at given void ratios. The results are plotted in Fig. 14, with both the V_s and the effective confinement in logarithmic scale. A power regression of the data confirms the power relation between the shear wave velocity and the effective confinement of the granular material. These results suggest that the exponent of the vertical pressure increases as the void ratio increases, with the values ranging between 0.2 and 0.3, and an average value around 0.25.

Fig. 15 presents the linear plots of the shear wave velocity as a function of the void ratio, for normally consolidated and overconsoli-

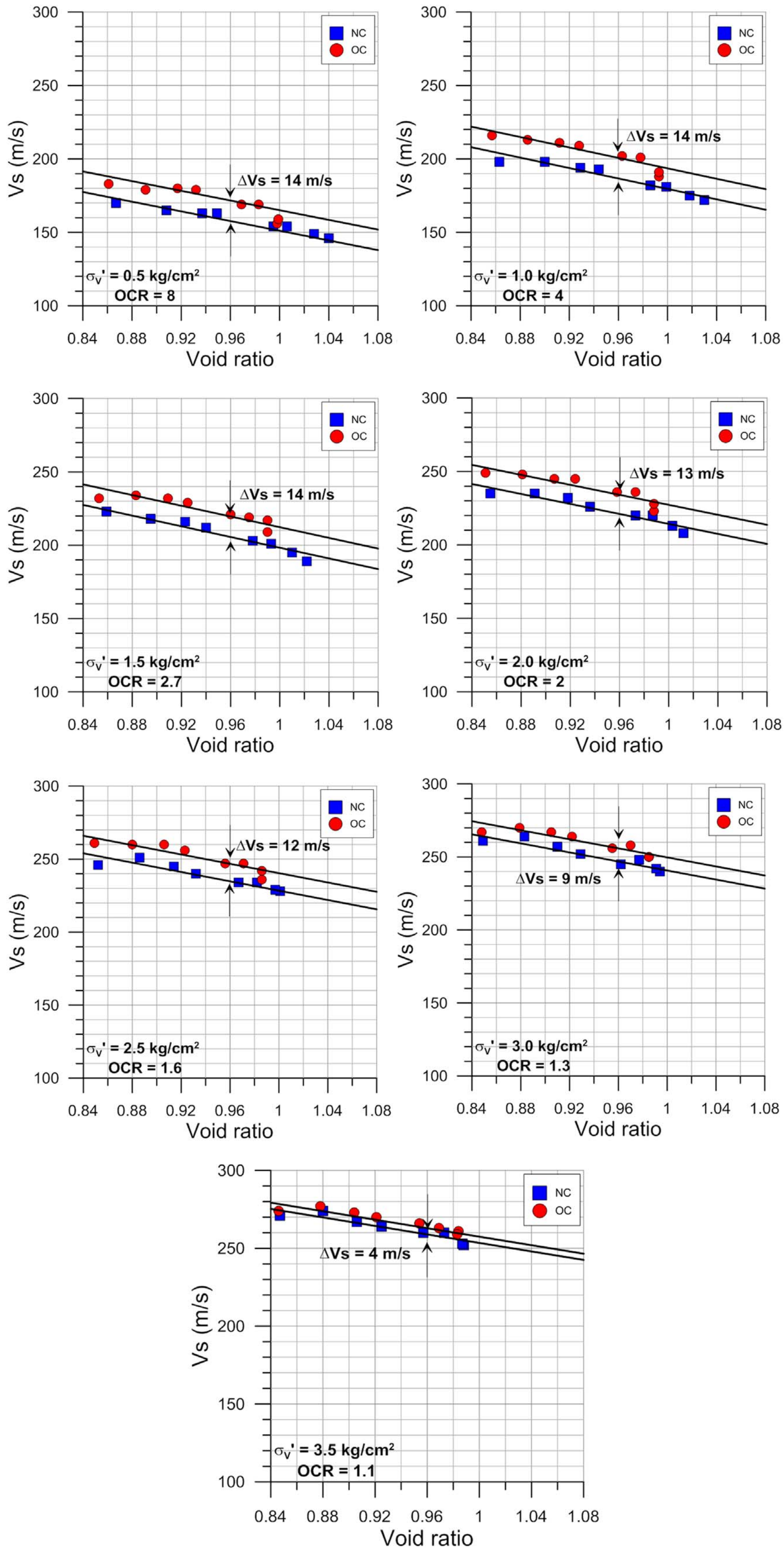

Fig. 19. Vs of Sand C measured at different confining pressure and overconsolidation ratios (1 kg/cm^2 to 100 kPa).

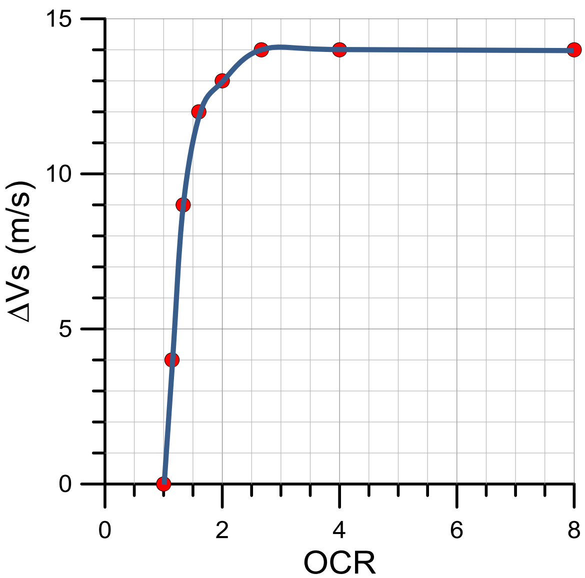

Fig. 20. Increment of shear wave velocity of Sand C due to overconsolidation.

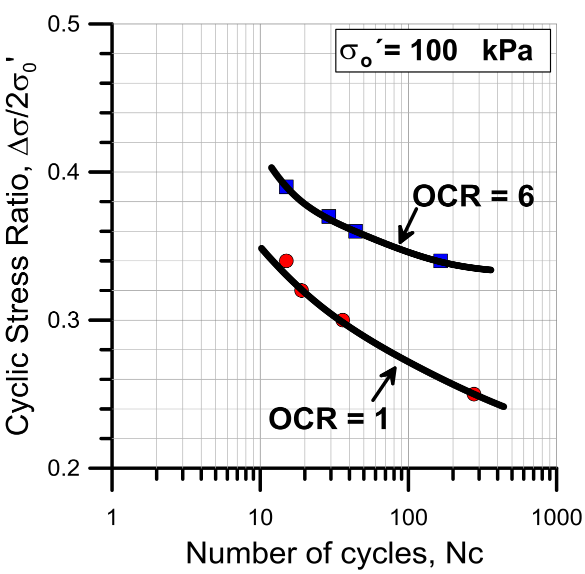

Fig. 21. Cyclic strength of normally and overconsolidated samples of Sand-C.

dated specimens of Sand-S, at different effective confinements and different overconsolidation ratios.

In addition to the previous observation related to the effect of the confinement, and the void ratio, on the shear wave velocity, it is observed that regardless of the effective confinement and the overconsolidation ratio, the shear wave velocity of overconsolidated specimens is higher than the shear wave velocity of normally consolidated specimens. Also, at a given OCR and vertical pressure, the difference between the shear wave velocity of overconsolidated specimens and normally consolidated specimens is approximately constant, regardless of the sample void ratio.

Fig. 16 shows the results in terms of the increment of the shear wave velocity at different overconsolidation ratios. It is observed that the shear wave velocity increases with the overconsolidated ratio. The plot of this increase, however, suggests that the increment of the shear wave velocity rapidly reaches a plateau for overconsolidation ratios higher than 8. In this particular case, for overconsolidation ratios of over 8, the increment would be less than 30 m/s.

For Sand-C, a similar interpretation of the results presented in Figs. 17–20 can be done. In the case of the effect of overconsolidation, the trends follow a pattern similar to that of Sand-S, with V_s marginally increasing; less than 15 m/s for overconsolidation ratios higher than 4.

The results presented above provide reliable evidence for the low sensitivity of V_s to the overconsolidation ratio.

9. Effect of overconsolidation on the cyclic strength of sands

An experimental program that considered the performance of undrained cyclic triaxial tests was carried out on both normally consolidated (NC) and overconsolidated (OC) specimens of Sand-C (Sanchez, [53]). These specimens were prepared initially with relative densities in the order of 67%. The NC specimens were isotropically consolidated at an effective confining stress of 1 kg/cm^2. The OC specimens were isotropically loaded to a confining pressure of 600 kPa (6 kg/cm^2) initially. Afterwards, the specimens were unloaded to an isotropic effective stress of 100 kPa. Therefore, the cyclic triaxial tests on these specimens were performed with an overconsolidation ratio of 6.

Fig. 21 presents the plot of the cyclic stress ratio, in linear scale, as a function of the number of cycles to liquefaction, in logarithmic scale. The liquefaction criterion used in these tests was based on deformations, as the number of cycles at which the axial deformation of the sand specimens reached a 5% of axial strain in double amplitude.

A significant effect of the overconsolidation ratio on the liquefaction resistance is observed. For a number of cycles in the range of 20–30, overconsolidated specimens (OCR=6) present a cyclic resistance approximately 20% higher than normally consolidated specimens. The increase is greater as the number of cycles increases. The experimental results obtained from the undrained cyclic tests suggest that the effect of the overconsolidation ratio on the cyclic strength is significant. This observation is in agreement with previous studies that already proved this well-known effect (Ishihara et al. [54]; Finn [55]; Dobry et al. [56]; Adalier et al. [57]).

10. Factors that have strong effect on liquefaction resistance but little effect on shear wave velocity

The main factors associated with the soil state that control, or have an important effect on the liquefaction resistance of sandy soil deposits are the following: relative density, soil structure or fabric (sample preparations methods), aging, overconsolidation, K_o (lateral pressure), seismic prestraining or preshaking. It is safe to say that there is a general consensus about the importance of these factors on the onset of liquefaction (Seed [58], Finn [55]; Ishihara [20,59], Dobry [15]).

On the other hand, in sandy soils some of these factors have only a marginal effect on V_s. Specifically, V_s is weakly influenced by: soil structure or fabric (sample preparations methods), aging, overconsolidation and seismic prestraining or preshaking.

Tatsuoka et al. [60] carried out an extensive experimental program to investigate the effect of sample preparation on the shear modulus. The conclusion was that the shear modulus at small strain level is insensitive to the sample preparation method, including pouring, compacting, moistening, saturating, unsaturating, freezing and thawing. Similar conclusion regarding the insensitivity of V_s to sand fabric has been reported by Alarcon et al. [61]. Experimental test results of V_s obtained for two different sample preparation methods on Ottawa sand (water pluviation and moist tamping) are presented in Fig. 22 (Robertson et al. [62]). It can be seen that the relationship between the normalized shear wave velocity, V_{s1}, and void ratio is not affected by the different fabrics generated by these methods of sample preparation. Similar experimental results have been reported by Sawangsuriya et al. [63] as shown in Fig. 23, where the two sample preparation methods used clearly reproduce the same relationship between V_s and the applied isotropic effective confining stress. The same void ratio of 0.56 (relative density of 58%) was repeated by these methods.

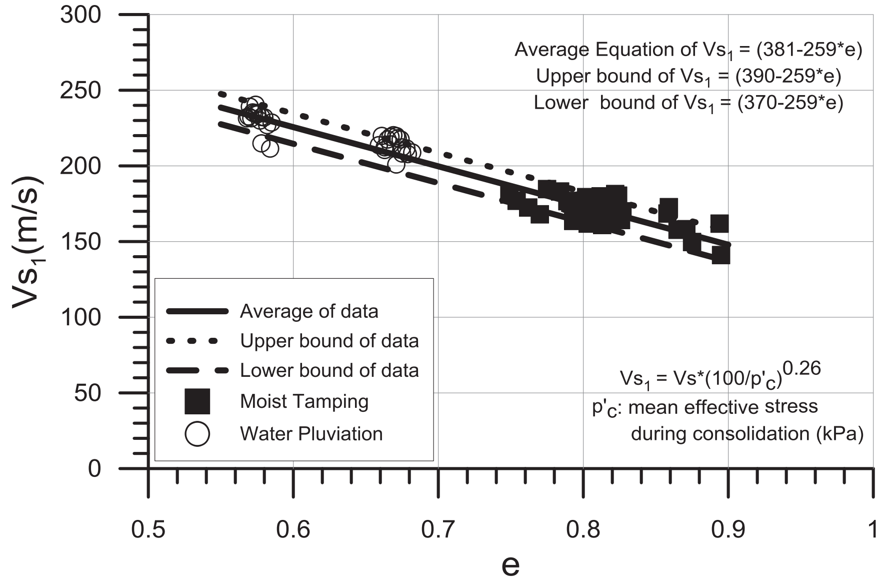

Fig. 22. Normalized shear wave velocity, V_{s1}, versus void ratio, e, for Ottawa sand during consolidation (modified from Robertson et al. [62]).

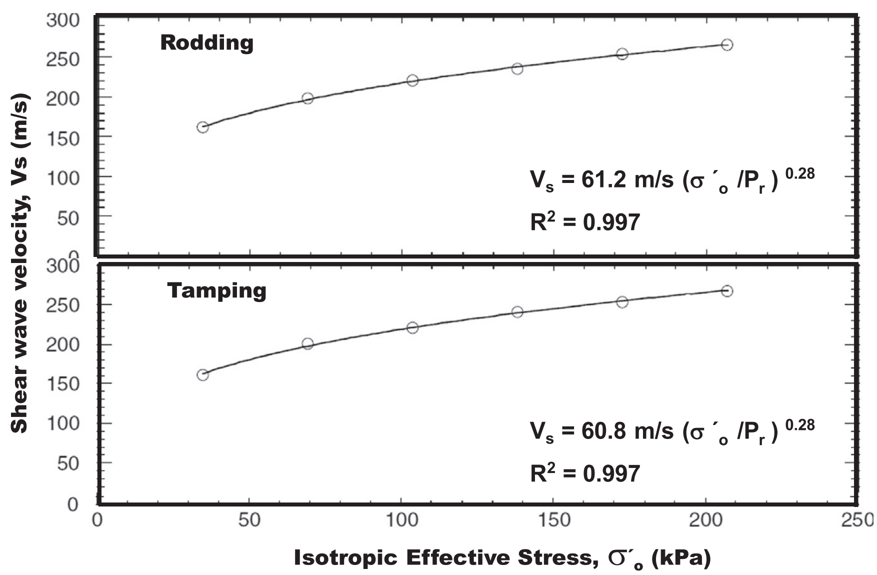

Fig. 23. Shear wave velocity for rodding and tamping sample preparation methods with a void ratio of 0.56 (from Sawangsuriya et al. [63]).

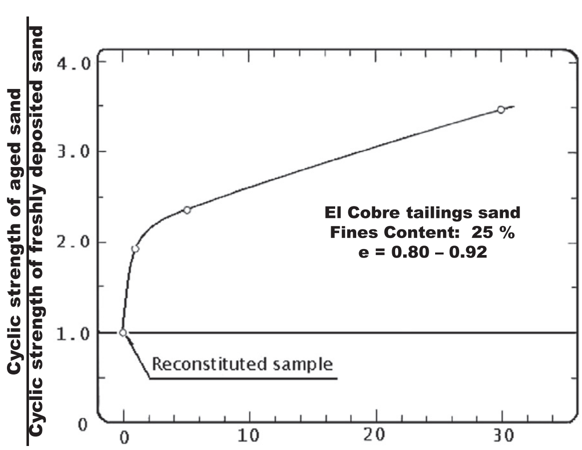

Fig. 24. Aging effect on the cyclic strength of tailing sands [67].

In contrast to the above, there is robust experimental evidence showing that the initial soil fabric, or sample preparation, has a significant effect on the onset of liquefaction (Park et al. [64]; Mulilis et al. [65]; Tatsuoka et al. [66]).

Aging is also a factor that has been reported to have an important effect on the cyclic strength of sandy soils (Troncoso et al. [67]; Mori et al. [68]). Experimental results on tailings sands, as shown Fig. 24, indicate that the cyclic stress ratio required for generating 5% strain in double amplitude increases by a factor of 3.5 in just 30 years of sustained deposition (Troncoso et al. [67]). On the other hand, Afifi et al. [69] have reported for sandy soils a relatively unimportant increase with time of the shear modulus at small strain level, G_{max}. The experimental results reported by Afifi et al. show a phase in which G_{max} increases about linearly with the logarithm of time. This phase, referred as the long-term time effect, takes place after completion of primary consolidation. The increase of the shear modulus over one logarithm cycle of time, ΔG, normalized by the value of shear modulus measured after 1000 min of application of constant confining pressure, G_{1000}, has been used as a good indicator of how aging increases G_{max} within one logarithmic cycle of time. For different type of soils, the aging effect on

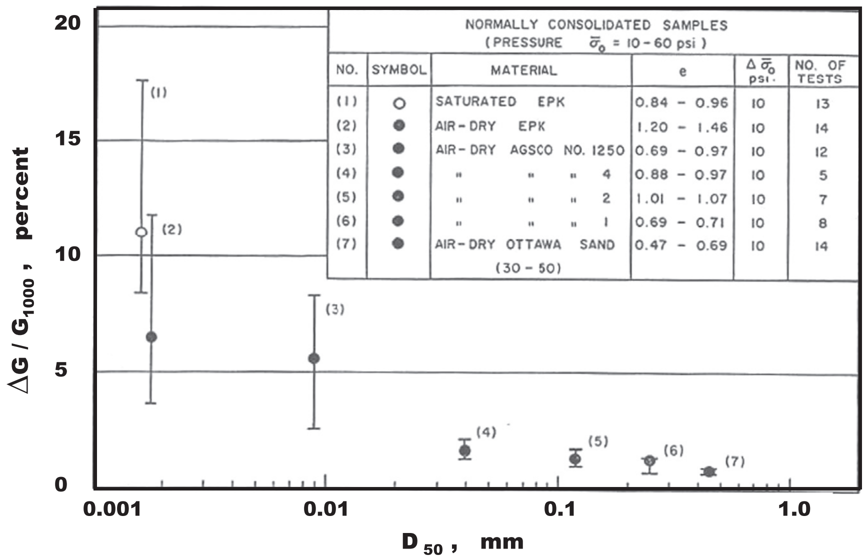

Fig. 25. Ratio of the shear modulus increment over one logarithm cycle of time and shear modulus measured after 1000 min of constant confining pressure, for different soils represented by their D_{50} ([69]).

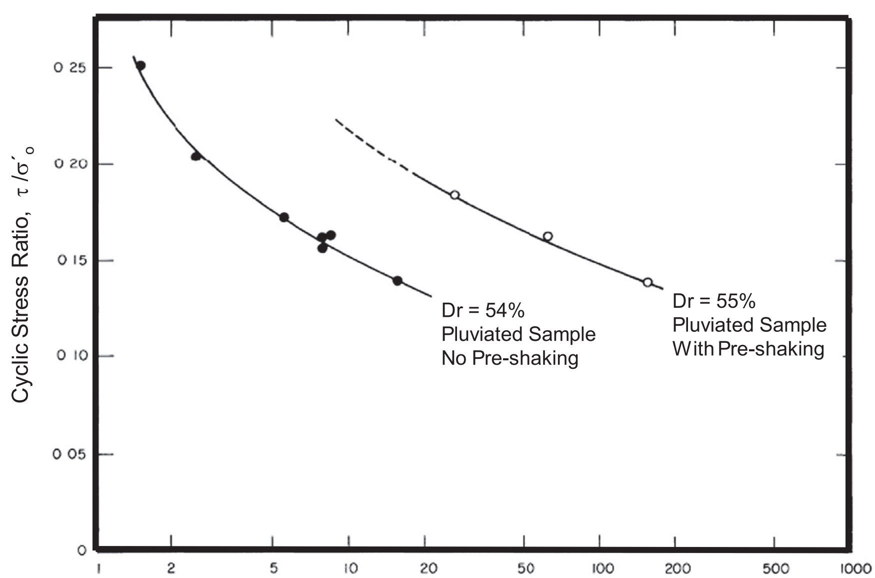

Fig. 26. Effect of pre-shaking on liquefaction resistance of sand [72].

G_{max} is summarized in Fig. 25. Afifi et al. [69] concluded that for soils with D_{50} particle size larger than 0.04 mm, the percent increase per log cycle is less than 3%, which is considered unimportant. Therefore, the effect of aging on V_s is even less, considering that $V_s=(G_{max}/\rho)^{0.5}$. Anderson et al. [70] have reported similar results confirming the negligible effect of aging on G_{max}, and therefore, on V_s.

Seismic pre-straining or strain history is also a factor that has an important effect on the liquefaction characteristics as it has been largely recognized (Finn et al. [71], Seed et al. [72], Dobry [15]). Natural sandy soil deposits are always exposed to small local seismic events that induce small cyclic straining, which causes a soil particle arrangement, or minor adjustments at grain contacts, although the variation of the soil density is negligible. Experimental test results confirming the effect of the strain history on the liquefaction resistance has been reported by Seed et al. [72], as shown Fig. 26. It is observed that the applied pre-shaking increases significantly the cyclic strength of the tested sand, which cannot be attributed to the marginal increase of the relative density of the specimens from 54% to 55%. However, there is experimental evidence suggesting that the pre-strain has little effect on the shear modulus at small strains (Drnevich et al. [73,74]; Witchmann et al. [75]), and thus on V_s. Experimental data reported by Drnevich el al. [73] are plotted in Fig. 27 to show the increment of the shear modulus due to the application of a pre-shaking of 1000 cycles at predetermined amplitude of shear strain. As can be seen, when pre-shaking of 1000 cycles of low-amplitude shear strain (1.6×10^{-2}%) is applied, the shear modulus at small strain is not affected. When pre-shaking of 1000 cycles of high-amplitude shear strain (6×10^{-2}%) is applied, the shear modulus at small strain increases at about 20%, which means an increment of less than 10% in the shear wave velocity.

Recently, El-Sekelly et al. [76] have reported centrifuge test results where the influence of preshaking on the liquefaction potential of silty sand deposits was investigated. One of the main findings was that the observed increase in liquefaction resistance with the number of earthquakes is not reflected in a corresponding increase in the shear wave velocity of the soil, as measured by bender elements throughout the test. Therefore, they concluded that the measured increased liquefac-

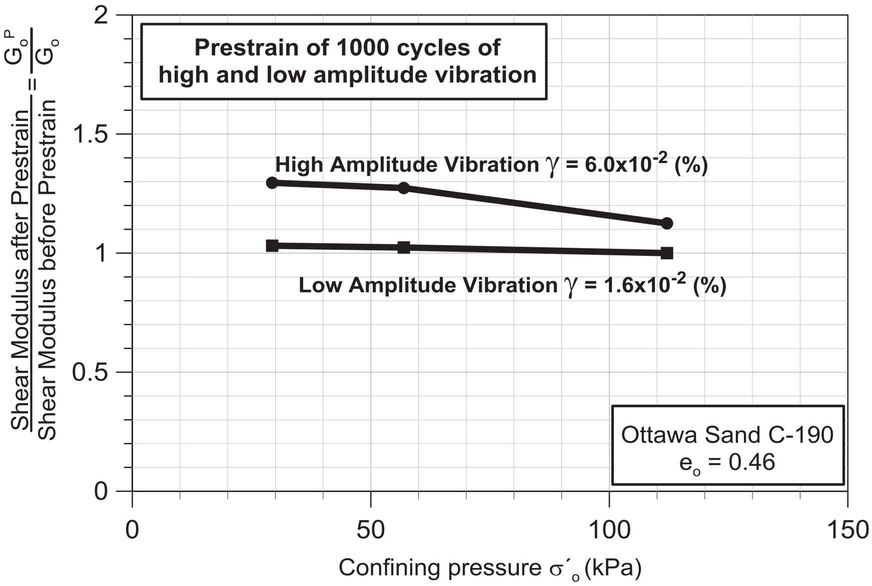

Fig. 27. Effect of cycles of prestrain on the low amplitude shear modulus (original data from Drnevich et al. [73]).

tion resistance is not predicted by the Vs-based liquefaction chart.

11. Concluding remarks

The shear strain thresholds that characterize the behavior of sandy soils have been described; especially important are the elastic threshold and the volumetric threshold shear strain. At very small shear strains, i.e. below 10^{-5} (10^{-3}%), the stress-strain response is fairly linear, and a shear strain level in the order of 10^{-4} (10^{-2}%), separates the cyclic soil response with and without volumetric strain accumulations.

The liquefaction phenomenon is intrinsically related to the natural tendency of loose cohesionless soils to generate positive volumetric strains (contraction) when subjected to monotonic or cyclic loads. Therefore, the onset of liquefaction takes place well above the volumetric threshold shear strain.

On the other hand, the measured shear wave velocity is a soil parameter essentially associated with a shear strain level in the elastic range, where the particle media do not show volumetric strains and only a marginal plastic strain.

The main factors with a significant impact on the liquefaction resistance of sandy soil deposits are: relative density, soil structure or fabric (sample preparation methods), aging, overconsolidation, Ko (lateral pressure), seismic prestraining or preshaking. However, among these factors, soil structure or fabric, aging, overconsolidation and seismic prestraining or preshaking have only a modest effect on V_s. Specifically, laboratory experimental results showing the low sensitivity of V_s to OCR are presented. Additionally, V_s correlates linearly with the void ratio, regardless of the maximum and minimum void ratios. In other words, V_s is unable to give information about the soil packing.

The Vs-based liquefaction chart presents a significant number of data that can be identified as false positives. Furthermore, when V_{s1} approaches to 200 m/s, CRR is highly sensitive to small changes in V_{s1}. Nevertheless, according to the reported data, there are no cases of liquefaction for $V_{s1} > 200$ m/s.

Shear wave velocity is an index parameter that can be measured in the field with relatively little effort compared to other field tests, and therefore, its use is highly tempting. Before surrendering to this temptation, engineers must be fully aware of the poor correlation between V_s and relative density and other limitations presented in this paper. When using shear wave velocity as a liquefaction predictor, it is recommended that the limitations described here are taken into account.

Acknowledgments

The author wants to acknowledge the very useful comments made by my colleagues, Dr. Felipe Ochoa and Mr. Gustavo Peters. Also, thanks are due to the Geotechnical Engineers of CMGI, Javiera Gonzalez, Guillermo Valladares, Gaspar Besio, and Sebastian Maureira, who have helped in the manuscript preparation. Special thanks to NGI and University of Chile where the presented tests were carried out. Many thanks are due to Dr. Laurence Wesley for his important comments and corrections.

References

[1] Youd TL, Idriss IM, Andrus RD, Arango I, Castro G, Christian JT, Dobry R, Finn WDL, Harder LF, Hynes ME, Ishihara K, Koester JP, Liao SSC, Marcuson WF, Martin GR, Mitchell JK, Moriwaki Y, Power MS, Robertson PK, Seed RB, Stokoe KH. Liquefaction resistance of soils: summary report from the 1996 NCEER and 1998 NCEER/NSF workshops on evaluation of liquefaction resistance of soils. J Geotech Geoenviron Eng ASCE 2001;127(4).

[2] Dobry R, Stokoe II, KH, Ladd RS, Youd TL. Liquefaction susceptibility from S-wave velocity. In: proceedings of ASCE national convention, in situ tests to evaluate liquefaction susceptibility. ASCE: New York; 1981.

[3] Robertson PK, Woeller DJ, Finn WDL. Seismic CPT for evaluating liquefaction potential. Can Geotech J 1992;29:686–95.

[4] Andrus RD, Stokoe II KHI. Liquefaction resistance based on shear wave velocity. In: proceedings of NCEER workshop on evaluation of liquefaction resistance of Soils, National Center for Earthquake Engineering Research, State University of New York at Buffalo; 1997. p. 89–128.

[5] Andrus RD, Stokoe KH. II, Liquefaction resistance of soils from shear wave velocity. J Geotech Geoenviron Eng 2000;126(11):1015–25.

[6] Andrus RD, Paramanthan P, Ellis BS, Zhang J, Juang CH. Comparing liquefaction evaluation methods using penetration-V_s relationships. Soil Dyn Earthq Eng 2004;24:713–21.

[7] Dobry R. Comparison between Clean Sand Liquefaction Charts Based on Penetration Resistance and Shear Wave Velocity. In: Prakash S, (Ed.). Proceedings of the 5th international conference on recent advances in geotechnical earthquake engineering and soil dynamics and symposium in honor of Prof. I.M. Idriss. San Diego, CA, Paper No. IMI4; 2010.

[8] Jamiolkowski M, LoPresti D. Discussion of correlation between liquefaction resistance and shear wave velocity by K. Tokimatsu and A. Uchida. Soils Found 1992;32(2):145–8.

[9] Verdugo R. Discussion of correlation between liquefaction resistance and shear wave velocity by K. Tokimatsu and A. Uchida. Soils Found 1992;32(2):144–5.

[10] Tatsuoka F, Sato T, Park C, Kim Y, Mukabi J, Kohata Y. Measurements of elastic properties of geomaterials in laboratory compression tests. ASTM Geotech Test J 1994;17(1):80–94.

[11] Kokusho T. Cyclic triaxial test of dynamic soil properties for wide strain range. Soils Found 1980;20:45–60.

[12] Dobry R, Ladd RS, Yokel FY, Chung RM, Powell D. Prediction of pore water pressure buildup and liquefaction of sands during earthquakes by the cyclic strain method. NBS Building Science Series 138, National Bureau of Standards:

Gaithersburg, Maryland; 1982.
[13] Dyvik R, Dobry R, Thomas G, Pierce W. Influence of consolidation shear stresses and relative density on threshold strain and pore pressure during cyclic straining of saturated sands. GL-84-15, Department of the Army, US Army Corps of Engineers; 1984.
[14] Vucetic M. Cyclic threshold shear strains in soils. J Geotech Eng ASCE 1994;120:2208–28.
[15] Dobry R, Abdoun T. An investigation into why liquefaction charts work: a necessary step toward integrating the states of art and practice. In: Ishihara Lecture. Proceedings of the 5th international conference on earthquake geotechnical engineering. Santiago, Chile; 2011.
[16] Ishihara K. Strength of cohesive soils under transient and cyclic loading conditions. In: Ergunay , Erdik , editors. State-of-the-Art in Earthquake Engineering. Turkish National Committee on Earthquake Engineering; 1981. p. 154–69.
[17] Ishihara K. Evaluation of soil properties for use in earthquake response analysis. In: Proceedings of international symposium on numerical models in geomechanics. Zurich; 1982. p. 237–59.
[18] Towhata I. Effects of Stress Axes Rotation on Deformation of Sand Undergoing Cyclic Shear. Thesis for Doctor of Engineering, University of Tokyo. March, 1982 [In Japanese].
[19] Casagrande A. Liquefaction and cyclic deformation of sands-a critical review. In: proceedings of the fifth panamericanconference on soil mechanics and foundation engineering. Buenos Aires, Argentina; 1975.
[20] Ishihara K. Liquefaction and flow failure during earthquakes. Geotechnique 1993;43(3):351–415, [33rd Rankine Lecture].
[21] Verdugo R. Characterization of sandy soil behavior under large deformations [Ph.D. Thesis]. University of Tokyo; 1992.
[22] Verdugo R, Ishihara K. The steady state of sandy soils. Soils Found 1996;36(2):81–91.
[23] Verdugo R, Bard E, Zavala G. Standard penetration tests on saturated sandy soils. In: proceedings of the X panamerican conference on soil mechanics and foundation engineering. México; 1995 [In Spanish].
[24] Seed HB, Tokimatsu K, Harder LF, Jr., Chung R. Influence of SPT procedures in soil liquefaction resistance evaluations. J Geotech Eng ASCE 1985;111(12):1425–45.
[25] Kishida H. Damage to reinforced concrete buildings in Niigata city with special reference to foundation engineering. Soils Found Jpn Soc Soil Mech Found Eng 1966;6(1):71–86.
[26] Ohsaki Y. Niigata Earthquakes, 1964, building damage and soil conditions. Soils Found 1966;6(2):14–37.
[27] Seed HB, Idriss IM, Arango I. Evaluation of liquefaction potential using field performance data. J Geotech Eng 1983;109.
[28] Seed HB, Tokimatsu K, Harder LF, Chung RM. The influence of SPT procedures in soil liquefaction resistance evaluations. Earthquake Engineering Research Center Report No. UCB/EERC-84/15. University of California at Berkeley; 1984.
[29] Cetin KO, Seed RB, Der Kiureghian A, Tokimatsu K, Harder LF, Kayen RE, Moss RES. Standard penetration test-based probabilistic and deterministic assessment of seismic soil liquefaction potential. J Geotech Geoenviron Eng ASCE 2004;130(12):1314–40.
[30] Boulanger RW, Wilson DW, Idriss IM. Examination and re-evaluation of SPT-based liquefaction triggering case histories. J Geotech Geoenviron Eng ASCE 2012;138:898–909.
[31] Boulanger RW, Idriss IM. CPT and SPT based liquefaction triggering procedures. Report No. UCD/CGM-14/01. University of California at Davis; 2014.
[32] Gibbs HJ, Holtz WG. Research on determining the density of sands by spoon penetration testing. In: Proceedings of the IV ICSMFE; 1957. p. 35–39.
[33] Cubrinovski M, Ishihara K. Empirical correlation between SPT N-value and relative density for sandy soils. Soils Found 1999;39(5):61–71.
[34] Skempton AW. Standard penetration test procedures and the effects in sands of overburden pressure, relative density, particle size, ageing and over consolidation. Geotechnique 1986;36(3).
[35] Seed HB, Idriss IM. Ground motions and soil liquefaction during earthquakes. Oakland, Calif: Earthquake Engineering Research Institute Monograph; 1982.
[36] Kayen RE, Mitchell JK, Seed RB, Lodge A, Nishio S, Coutinho R. Evaluation of SPT-, CPT-, and shear wave-based methods for liquefaction potential assessment using Loma Prieta data. In: proceedings of the 4th Japan-U.S. workshop on earthquake-resistant design of lifeline fac. and countermeasures for soil liquefaction; Vol. 1; 1992. p. 177–204.
[37] Jamiolkowski M, Ghionna V, Lancellota R, Pasqualini E. New correlations of penetration tests for design practice. in: Proceedings of ISOPT-1; 1988; Vol 1, p. 263–95.
[38] Stark TD, Olson SM. Liquefaction resistance using CPT and field case histories. J Geotech Eng ASCE 1995;121(12):856–69.
[39] Robertson PK, Wride CE. Evaluating cyclic liquefaction potential using the cone penetration test. Can Geotech J 1998;35(3):442–59.
[40] Suzuki Y, Tokimatsu K, Moss RES, Seed RB, Kayen RE. CPT-based liquefaction case histories from the 1995 Hyogoken-Nambu (Kobe) earthquake, Japan. Geotechnical engineering research report No. UCB/GE-2003/03; May 2003.
[41] Idriss IM, Boulanger RW. Semi-empirical procedures for evaluating liquefaction potential during earthquakes. In: Proceedings of the 3rd international conference on earthquake geotechnical engineering. Berkeley, USA; 2004.
[42] Schmertmann JH. Guidelines for cone penetration test, performance and design. U. S. Department of Transportation Federal Highway Administration. Report FHWA-TS-78-209; 1978.
[43] Lunne T, Christoffersen H. Interpretation of cone penetrometer data for offshore sands. In: Proceedings of the 15th Offshore Technology Conference, USA; 1983; Vol. 1, p. 181–92.
[44] Baldi G, Bellotti R, Ghionna N, Jamiolkowski M, Pasqualini E. Interpretation of CPT's and CPTU's. 2nd Part: Drained penetration of sands. In: proceedings of the fouth international geotechnical seminar field instrumentation and in-situ measurements. Singapore; 1986; p. 143–56.
[45] Robertson PK, Campanella RG. Interpretation of cone penetration tests; part I and II. Can Geotech J 1983;20(4):718–45.
[46] BellotiR, GhionnaV, JamiolkowskiM, LancellottaR. Shear strength from CPT. In: proceedings of ICSMFE. Rio de Janeiro; 1989.
[47] Jamiolkowski M, LoPresti D, Manassero M. Evaluation of relative density and shear strength of sands from cone penetration test and flat dilatometer test. Soil Behavior and Soft Ground Construction (GSP 119), ASCE, Reston/VA. 2001. p. 201–38.
[48] Roesler S. Anisotropic shear modulus due to stress anisotropy. J Geotech Eng Div ASCE 1979;105(GT7).
[49] Stokoe KH, Lee SH, Knox DP. Shear moduli measurements under true triaxial stresses. In: proceedings advances in the art of testing soils under cyclic conditions. ASCE; 1985. p. 166–85.
[50] Belloti R, Jamiolkowski M, Lo Presti DC, O´Neill DA. Anisotropy of small strain stiffness in Ticino sand. Geotechnique 1996;46(1):115–31.
[51] Hardin BO, Richart FE. Elastic wave velocities in granular soils. Soil Mech Found Div ASCE 1963;89:33–65.
[52] Dyvik R, Madshus C. Lab Measurements of Gmax Using Bender Elements. In: proceedings of the geotechnical engineering division: advances in the art of testing soil under cyclic conditions. ASCE, Detroit, MI; 1985. p. 186–96.
[53] Sanchez A. Undrained steady state strength of sands: initial state and its correlation with the steady state through the shear wave velocity (civil engineering thesis). [In Spanish]: University of Chile; 2002.
[54] Ishihara K, Takatsu H. Effects of overconsolidation and Ko conditions on the liquefaction characteristic of sands. Soils Found 1979;19(4):59–68.
[55] Finn L. Liquefaction potential: developments since 1976. In: proceedings of international conference on recent advances in earthquake engineering and soil dynamic; 1981. p. 655–81.
[56] Dobry R, Yokel FY, Ladd RS.Liquefaction Potential of overconsolidated sands in areas with moderate seismicity. In: Beavers JE (Ed.). Earthquakes and Earthquake Engineering: The Eastern United States; 1981b; Vol. 2, p. 642–64.
[57] Adalier K, Elgamal A. Liquefaction of over-consolidated sand: a centrifuge investigation. J Earth Eng 2005;9:127–50.
[58] Seed HB. Soil liquefaction and cyclic mobility evaluation for level ground during earthquakes. J Geotech Eng Div ASCE 1979;105(GT2):201–55.
[59] Ishihara K. Stability of natural deposits during earthquakes. In: proceedings of the 11th international conference on soil mechanics and foundation engineering. San Francisco, USA; 1985.
[60] Tatsuoka F, Iwasaki T, Yoshida S, Fukushima S, Sudo H. Shear modulus and damping by drained tests on clean sand specimens reconstituted by various methods. Soils Found 1979;19(1):39–54.
[61] Alarcon-Guzman A, Chameau J, Leonards G, Frost J. Shear modulus and cyclic undrained behavior of sands. Soils Found 1989;29(4):105–19.
[62] Robertson P, Sasitharan S, Cunning J, Sego D. Shear-wave velocity to evaluate in-situ state of ottawa sand. J Geotech Eng 1995;121(3):262–73.
[63] Sawangsuriya A, Fratta D, Bosscher PJ, Edil TB. S-wave velocity stress power relationship: packing and contact behavior of sand specimens. Geo-Denver Conference, Advances in Measurement and Modeling of Soil Behavior, ASCE, Geotechnical Special Publication, No.173; 2007.
[64] Park TK, Silver ML. Dynamic triaxial and simple shear behavior of sand. J Geotech Eng Div ASCE 1975;101(GT6):513–29.
[65] Mulilis JP, Chan CK, Seed HB. The effects of method of sample preparation on the cyclic stress-strain behavior of sands. Report No. EERC 75-18, EERC, University of California, Berkeley; 1975.
[66] Tatsuoka F, Toki S, Miura S, Kato H, Okamoto M, Yamada S, Yasuda S, Tanizawa F. Some factors affecting cyclic undrained triaxial strength of sand. Soils Found 1986;26(3):99–116.
[67] Troncoso J, Ishihara K, Verdugo R. Aging effects on cyclic shear strength of tailings materials. In: proceedings of the IX world conference on earthquake engineering. Tokyo, Japan. 1988; Vol.3, pp. 121–26.
[68] Mori K, Seed HB, Chan CK. Influence of sample disturbance on sand response to cyclic loading. J Geotech Eng Div ASCE 1978;104(GT3):323–39.
[69] Afifi S, Richart Jr. Stress-history effects on shear modulus of soils. Soils Found 1973;13(1):77–95.
[70] Anderson DG, Stokoe K. II, Shear Modulus: a time-dependent soil property. Dyn Geotech Test ASTM STP 1978;654:66–90.
[71] Finn L, Bransby P, Pickering D. Effect of strain history on liquefaction of sands. J Soil Mech Found Div 1970;96(SM6):1917–34.
[72] Seed HB, Mori K, Chan C. Influence of seismic history on the liquefaction characteristics of sands. Report No. EERC 75-25, Earthquake Engineering Research Center. University of California: Berkeley; 1975.
[73] Drnevich V, Hall J, Richart F. Effects of amplitude of vibration on the shear modulus of sand. In: proceedings of international symposium on wave propagation and dynamic properties of earth mat.; 1967. p. 189–99.
[74] Drnevich VP, Richart FE. Jr., Dynamic prestraining of dry sand. J Soil Mech Found Div ASCE 1970;96(SM2):453–69.
[75] Witchmann T, Triantafyllidis T. Influence of a cyclic and dynamic loading history on dynamic properties of dry sand I: cyclic and dynamic torsional prestraining. Soil Dyn Earthq Eng 2004;24:127–47.
[76] El-Sekelly W, Dobry R, Abdoun T, Steidl J. Centrifuge modeling of the effect of preshaking on the liquefaction resistance of silty sand deposits. J Geotech Geoenviron Eng 2016, [Published online on February 29].